Electronic Supplementary Material (ESI) for Materials Chemistry Frontiers.

Supporting Information

Design for Multi-step Mechanochromic Luminescent Property by Enhancement of Environmental Sensitivity in the Solid-state Emissive Boron Complex

Satoru Saotome, Kazumasa Suenaga, Kazuo Tanaka and Yoshiki Chujo*

Department of Polymer Chemistry, Graduate School of Engineering, Kyoto University,

Katsura, Nishikyo-ku, Kyoto 615-8510, Japan

E-mail: tanaka@poly.synchem.kyoto-u.ac.jp

Phone: +81-75-383-2604

Fax: +81-75-383-2605

General

^{1}H (400 MHz), ^{11}B (128 MHz), and ^{13}C (100 MHz) NMR spectra were recorded on JEOL JNM-EX400 and JEOL JNM-AL400 spectrometers. In ^{1}H and ^{13}C NMR spectra, tetramethylsilane (TMS) was used as an internal standard in $CDCl_3$, and ^{11}B NMR spectra were referenced externally to $BF_3{\cdot}OEt_2$ (sealed capillary). High-resolution mass spectra (HRMS) were obtained by electron spray ionization (ESI) technique. UV−vis absorption spectra were recorded on a SHIMADZU UV-3600 spectrophotometer and photoluminescence (PL) spectra were measured with a HORIBA Fluorlog-3 spectrofluorometer using quartz cuvettes with a 1 cm optical path length. Photoluminescence quantum yields (QY) were measured with a Hamamatsu Photonics Quantaurus-QY Plus C13534-01 measurement device; excitation at 400 nm using a xenon lump. Fluorescence lifetime analyses were carried out on a HORIBA FluoreCube spectrofluorometer system; excitation at 375 nm using a UV diode laser (NanoLED-375L). Elemental analysis was performed at the Microanalytical Center of Kyoto University. Powder X-ray diffraction (PXRD) patterns were taken by using CuKα radiation with Rigaku Miniflex. X-ray crystallographic analyses were carried out by Rigaku R-AXIS RAPID-F graphite-monochromated Mo Kα radiation diffractometer with imaging plate. A symmetry-related absorption correction was carried out by using the program ABSCOR. The analysis was carried out with direct methods (SHELX-97 or SIR92) using Yadokari-XG and shelxle64. The program ORTEP35 was used to generate the X-ray structural diagram. Cyclic voltammetry (CV) was carried out on a BASALS-Electrochemical-Analyzer Model 600D with a Pt working electrode, a Pt counter electrode, an Ag/Ag^{+} reference electrode, and the ferrocene/ferrocenium external reference at a scan rate of 10 mVs^{-1}. Thermogravimetric analysis (TGA) was performed using a HITACHI STA 7200 instrument, with the heating rate of 10 °C/min. up to 900 °C under nitrogen atmosphere. DSC thermograms were carried out on a HITACHI DSC 7020 instrument. The sample on the aluminum pan was heated at the rate of 10 °C/min under nitrogen flowing (50 mL/min).

Synthesis of 2

A solution of 5-bromo-2-methyl-pyridine (1.53 g, 8.87 mmol) in THF (20 ml) was cooled at −78 °C under Ar atmosphere. To this stirred colorless solution was added dropwise lithium diisopropylamide (LDA) (1.1 mol/L in *n*-hexane and THF, 8.0 mL, 8.8 mmol) by a syringe over 120 min. After the mixture was stirred for 60 min, to this stirred red solution was added dropwise *N*-methoxy-*N*-methylbenzamide (1.20 mL, 8.06 mmol) by a syringe over 5 min. After the mixture was stirred for 200 min, the solution was allowed to warm to room temperature. Then the reaction was quenched by addition of water. The mixture was extracted with CH_2Cl_2 (4 × 100 mL). The combined organic layers were washed with water (2 × 100 mL) and brine (100 mL), and then dried over $MgSO_4$. After filtration, the solvent was removed with a rotary evaporator. The residue was purified by column chromatography on SiO_2 with *n*-hexane and ethylacetate (*n*-hexane/ethylacetate = 3/2) as an eluent to afforded **1** as a yellow solid. The solid was subjected to the next reaction without further purification.

This yellow solid **1** was dissolved in CH_2Cl_2 (40.0 mL) under Ar atmosphere. To this stirred solution was added trimethylamine (8.0 mL) and then dropwise $BF_3{\cdot}Et_2O$ (6.9 mL, 56 mmol) by a syringe. The mixture was heated to 60 °C and stirred overnight with reflux. After cooling to room temperature, the reaction was quenched by addition of water. The combined organic layers were washed with water (2 × 100 mL) and brine (100 mL), and then dried over $MgSO_4$. After filtration, the solvent was removed with a rotary evaporator. The residue was purified by column chromatography on SiO_2 with *n*-hexane and ethylacetate (*n*-hexane/ethylacetate = 3/2) as an eluent and recrystallization from ethanol to afforded **2** (607 mg, 1.87 mmol, 33%) as a yellow crystalline. ^{1}H NMR ($CDCl_3$): δ 8.53 (1H, s), 7.98 (1H, dd, J = 8.8, 2.2 Hz), 7.95 (2H, dd, J = 7.7, 1.6 Hz), 7.48 (3H, m), 7.23 (1H, d, J = 8.8 Hz), 6.37 (1H, s) ppm. ^{13}C NMR($CDCl_3$): δ 163.9, 150.5, 144.0, 141.0,

133.8, 131.3, 128.6, 126.6, 123.4, 114.4, 92.7 ppm. ^{11}B NMR ($CDCl_3$): δ 1.08 ppm. HRMS(ESI): Calcd for $[M+Na]^+$, 345.9821; found, m/z 345.9823.

Synthesis of FBKI-thio

The solution of **2** (100mg, 0.309 mmol), 2-(4,4,5,5-tetramethyl-1,3,2-dioxaborolan-2-yl)thiophene (71.3 mg, 0.400 mmol), [1,1'-bis(diphenylphosphino)-ferrocene]palladium(II) dichloride dichloromethane adduct (12.6 mg, 0.0154 mmol) and K_2CO_3 (427 mg, 3.09 mmol) in toluene (2.0 mL) and water (1.0 mL) was heated to 80 °C under Ar atmosphere overnight. After cooling to room temperature, the reaction was quenched by addition of water. The combined organic layers were washed with water (2 × 100 mL) and brine (100 mL), and then dried over $MgSO_4$. After filtration, the solvent was removed with a rotary evaporator. The residue was purified by column chromatography on SiO_2 with *n*-hexane and ethylacetate (*n*-hexane/ethylacetate = 3/2) as an eluent and recrystallization from ethanol to afforded FBKI-thio (76.6 mg, 0.234 mmol, 76%) as a yellow crystal. ^{1}H NMR ($CDCl_3$): δ 8.67 (1H, s), 8.09 (1H, dd, *J* = 8.6, 2.2 Hz), 7.95 (2H, dd, *J* = 7.6, 2.1 Hz), 7.47 (2H, d, *J* = 1.9 Hz), 7.45 (3H, m), 7.35 (1H, d, *J* = 8.6 Hz), 6.42 (1H, s) ppm. ^{13}C NMR($CDCl_3$): δ 163.0, 150.1, 138.4, 137.9, 136.6, 134.3, 131.2, 128.9, 128.7, 128.3, 127.2, 126.7, 125.2, 122.8, 93.2 ppm. ^{11}B NMR ($CDCl_3$): δ 1.51 ppm. HRMS(ESI): Calcd for $[M+Na]^+$, 350.0593 ; found, m/z 350.0592. Anal. Calcd for $C_{17}H_{12}BF_2NOS$: C, 62.41; H, 3.70; N, 4.28. Found: C, 62.41; H, 3.75; N, 4.13.

Mechanical treatments

Smashing: By using a metal spatula, the crystal powder was continuously tapped. After a few minutes, sample color was constant and then additional treatment was applied (total 5 min). The sample was used for the next grinding step.

Grinding: The sample was put into an agate mortar and ground with an agate pestle. After a while, sample color was constant and then additional treatment was applied (total **A**: 10 min, **B**: 20 min).

Reversibility evaluation: The samples were heated at 80 °C for 1 h.

NMR Spectra

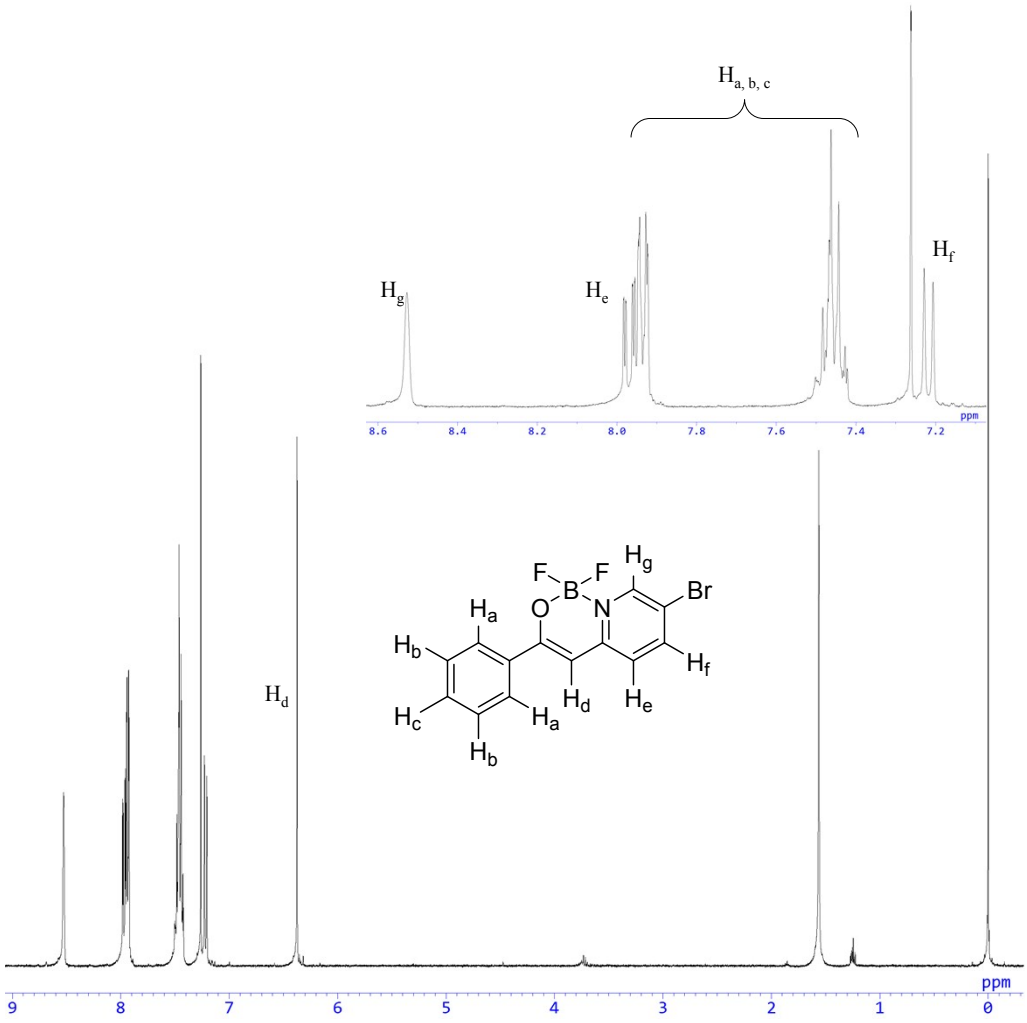

Chart S1. ^{1}H NMR spectrum of **2** in $CDCl_3$.

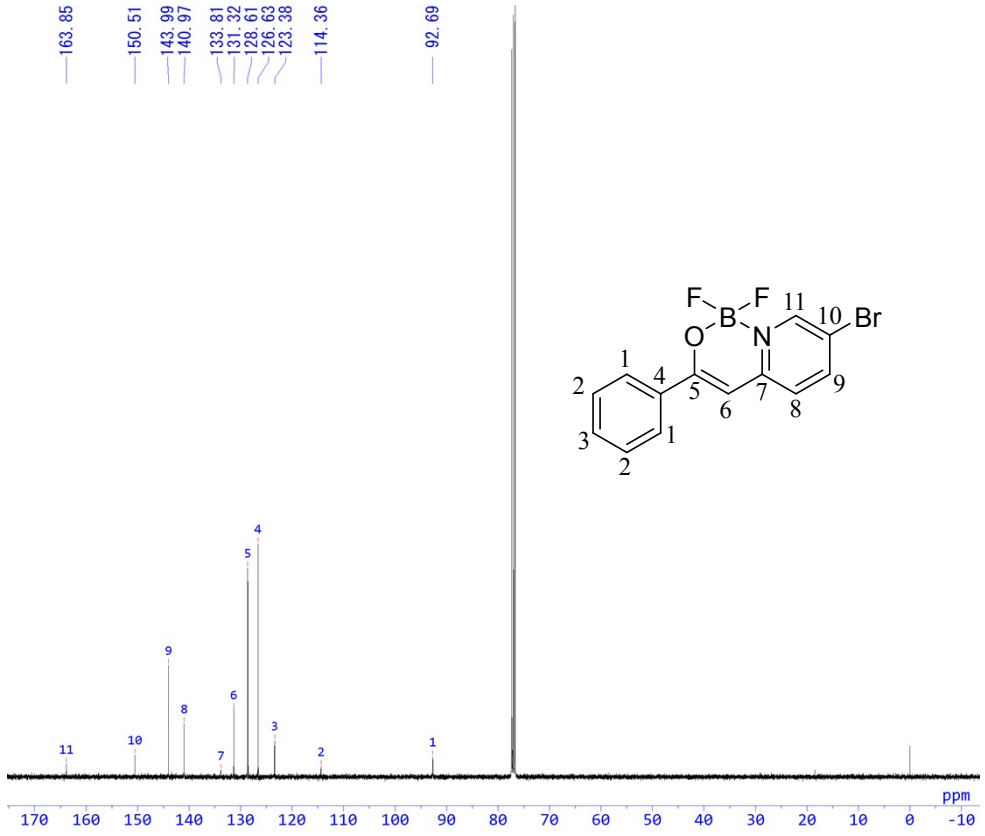

Chart S2. ^{13}C NMR spectrum of **2** in $CDCl_3$.

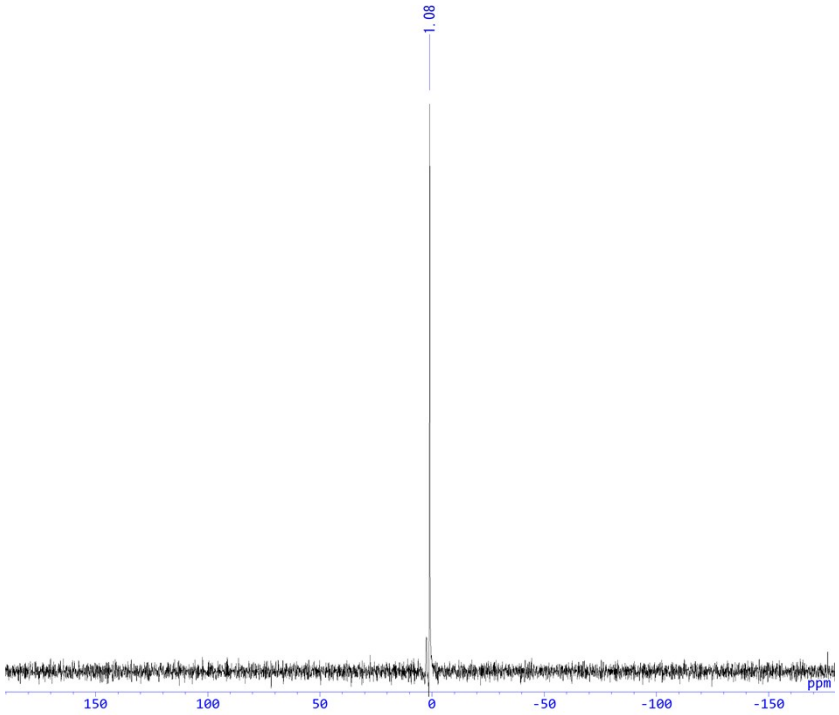

Chart S3. ^{11}B NMR spectrum of **2** in $CDCl_3$.

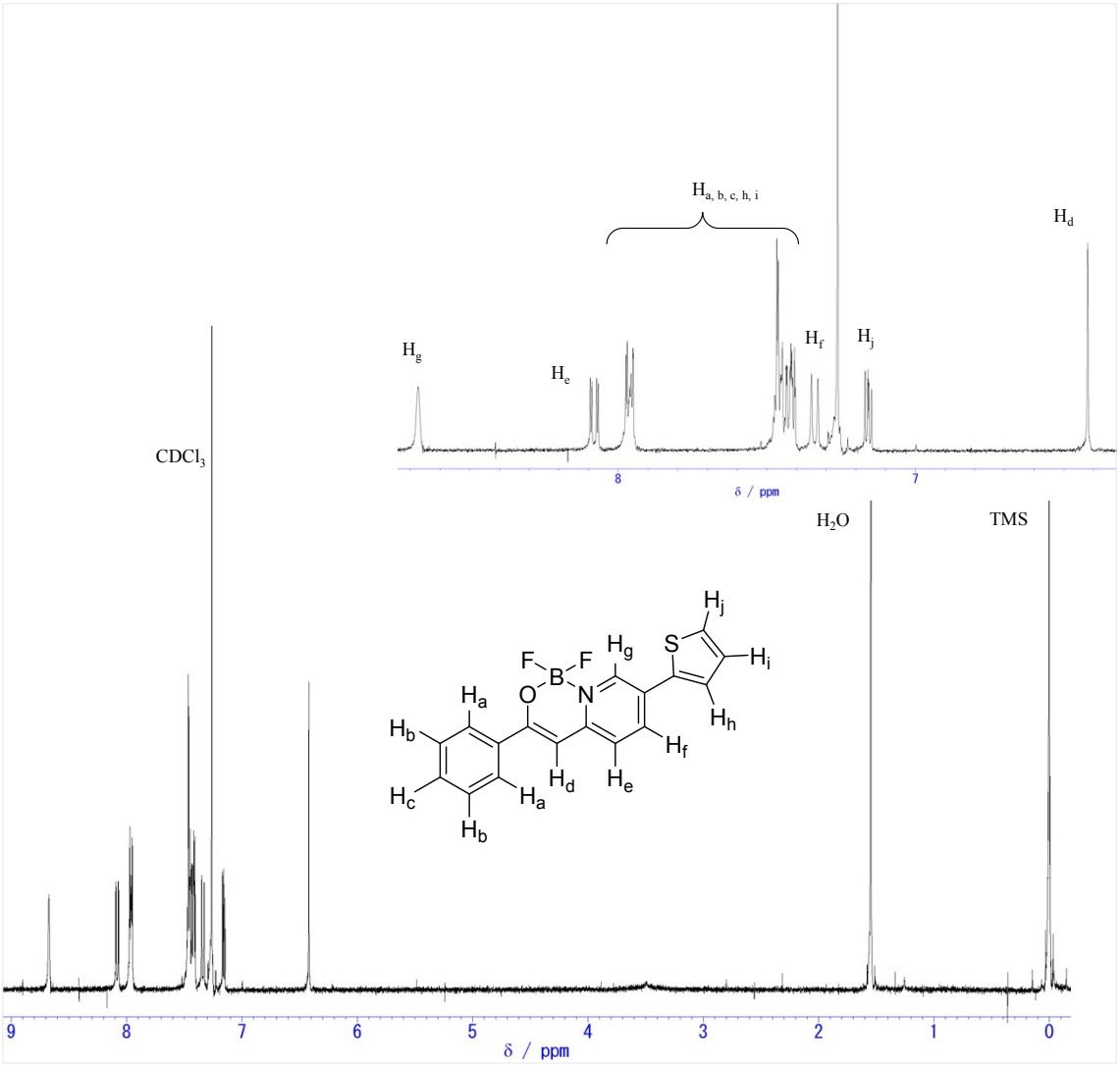

Chart S4 ^{1}H NMR spectrum of FBKI-thio in $CDCl_3$.

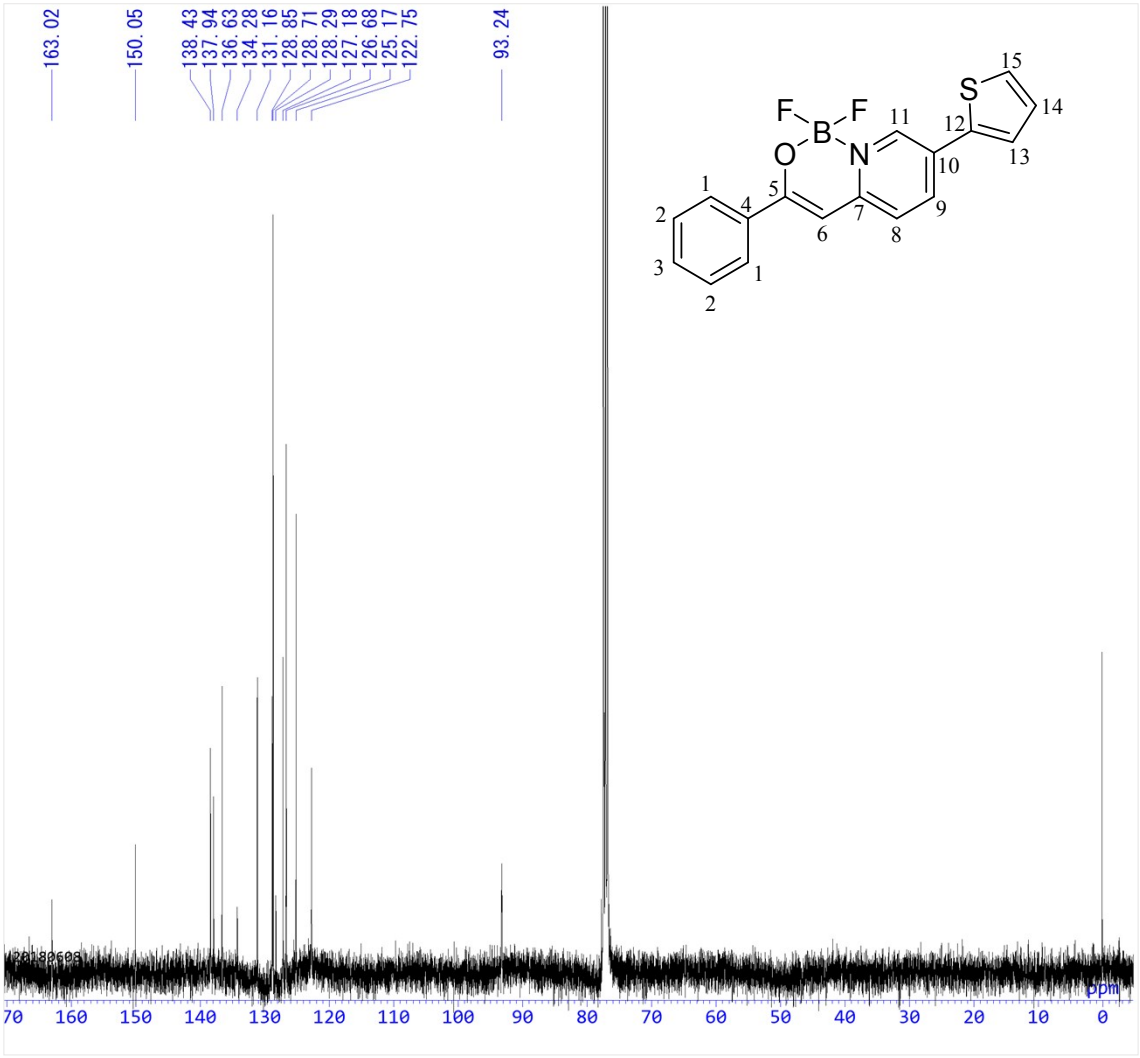

Chart S5. ^{13}C NMR spectrum of FBKI-thio in $CDCl_3$.

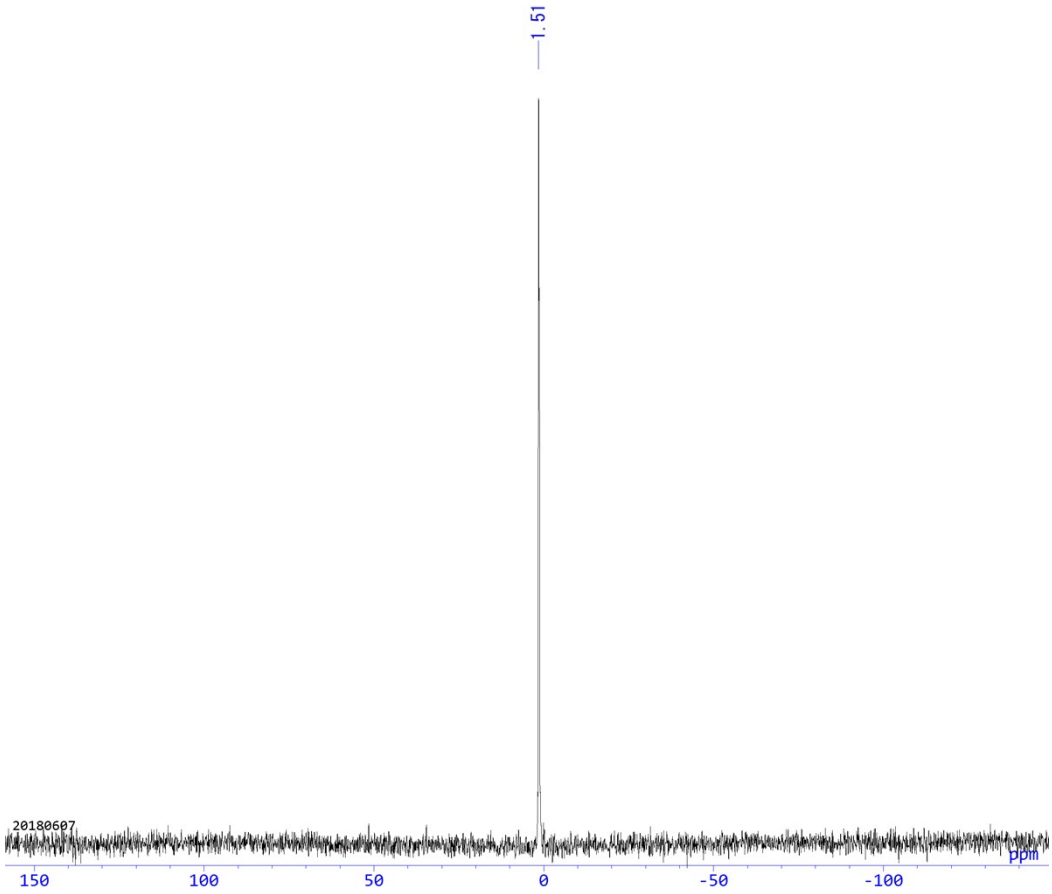

Chart S6. ^{11}B NMR spectrum of FBKI-thio in $CDCl_3$.

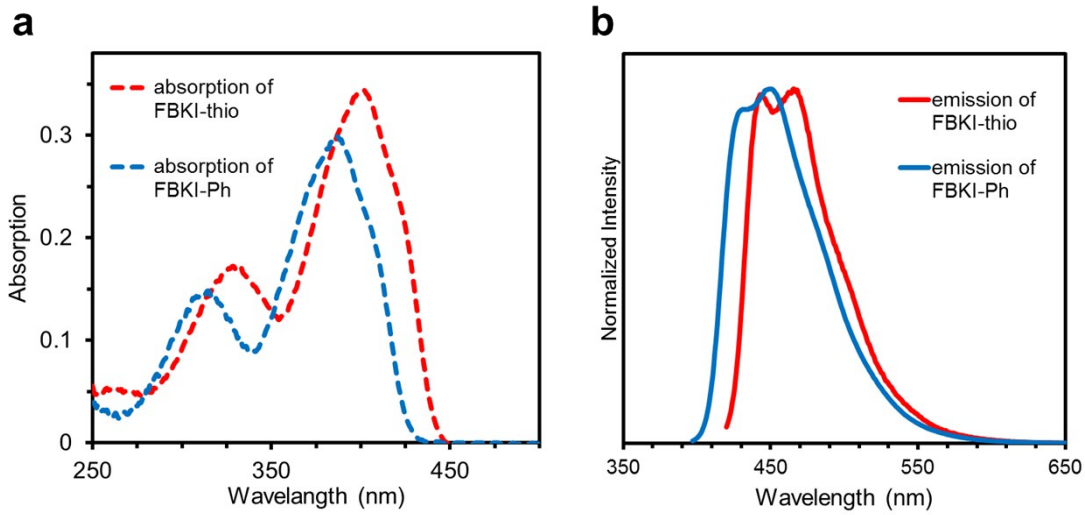

Figure S1. (a) UV−vis absorption and (b) photoluminescence spectra of FBKI and FBKI-thio in THF (1.0×10^{-5} M). Excitation wavelengths were at λ_{abs} (400 nm for FBKI-thio, 387 nm for FBKI).

Table S1. Optical properties of FBKI-thio and FBKI[a]

	λ_{abs} (nm)	ε ($M^{-1}cm^{-1}$)	λ_{em} (nm)[b]	Φ_{PL}[b]	τ (ns)[c]	k_r (10^9 s^{-1})	k_{nr} (10^9 s^{-1})
FBKI-thio	400	3.44×10^4	466	0.29	0.93 ($\chi^2 = 1.04$)	3.12	0.76
FBKI	387	3.33×10^4	450	0.17	0.50 ($\chi^2 = 1.01$)	3.40	1.66

[a] Measured in THF (1.0×10^{-5} M).

[b] Determined as an absolute value in the integration sphere.

[c] Excited at 375 nm.

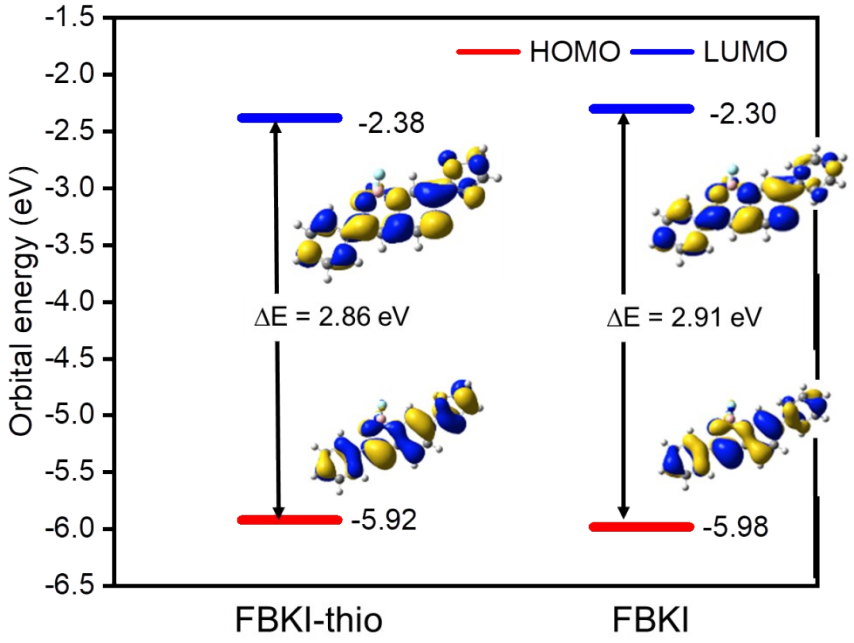

Figure S2. Structures and molecular orbital diagrams for the LUMO and HOMO of FBKI-thio (left) and FBKI (right) with the density functional theory method at B3LYP/6-311G(d, p)//B3LYP/6-311G(d, p) level.

Table S2. Electrochemical properties of the synthesized fused-boron ketoiminates[a]

	$E_{onset,\ ox}$ [V][b]	$E_{onset,\ red}$ [V][c]	E_{HOMO}^{CV} [eV][d]	E_{LUMO}^{CV} [eV][e]	E_{gap}^{CV} [eV][f]
FBKI-thio	0.91	–1.95	–6.01	–3.15	2.86
FBKI	1.17	–1.74	–5.74	–2.83	2.91

[a] Determined form cyclic voltammogram in CH_2Cl_2 (1×10^{-3} M) with 0.1 M Bu_4NPF_6 as a supporting electrolyte, Ag/AgCl as a reference electrode, Pt as working and counter electrodes, and a ferrocene/ferrocenium external standard at room temperature with a scan rate at 100 mV/s under Ar. [b]Estimated from the onset of the oxidation wave (vs Fc/Fc^+). [c]Estimated from the onset of the reduction wave (vs Fc/Fc^+). [d]$E_{HOMO}^{CV} = -4.8 - E_{onset,ox}$. [e]$E_{LUMO}^{CV} = -4.8 - E_{onset,red}$. [f]$E_{gap}^{CV} = E_{LUMO}^{CV} - E_{HOMO}^{CV}$.

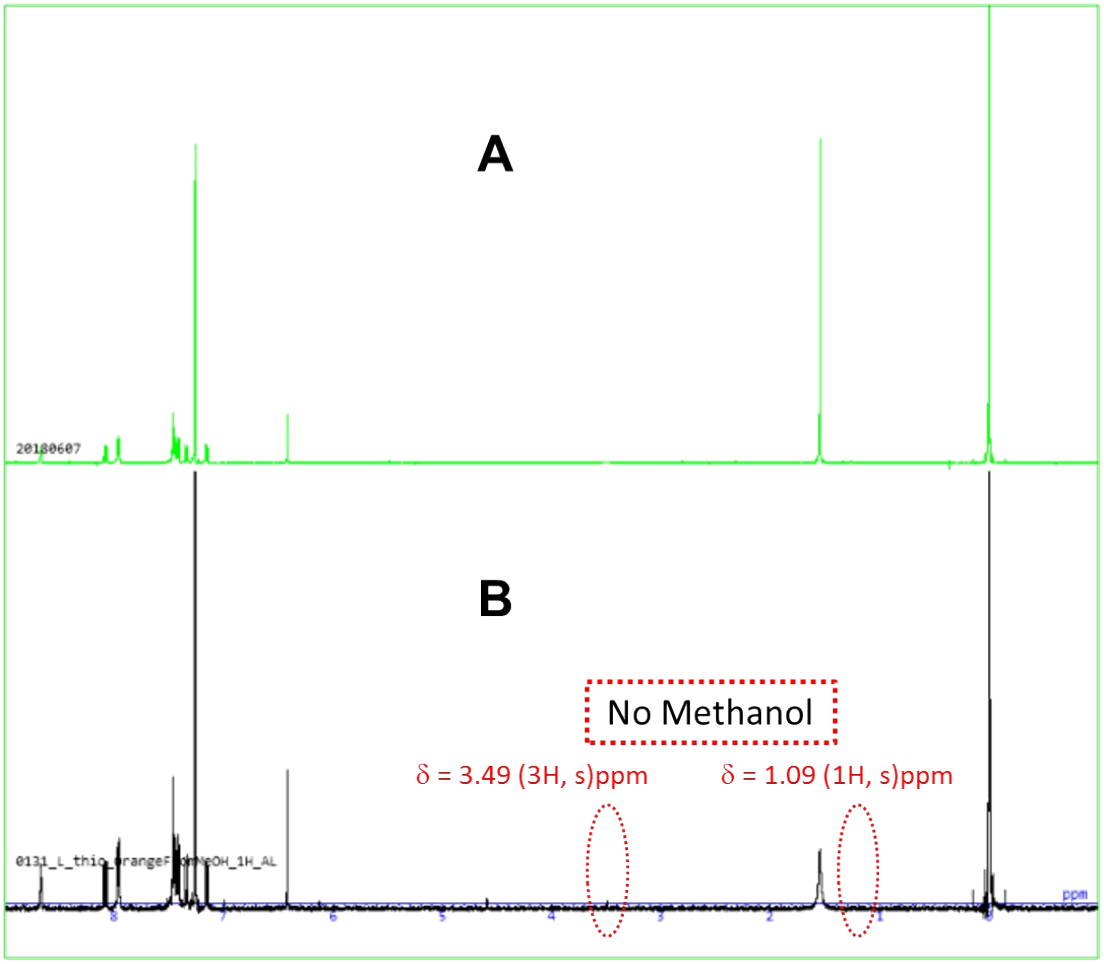

Figure S3. ^{1}H NMR spectra of crystals **A** and **B** in $CDCl_3$.

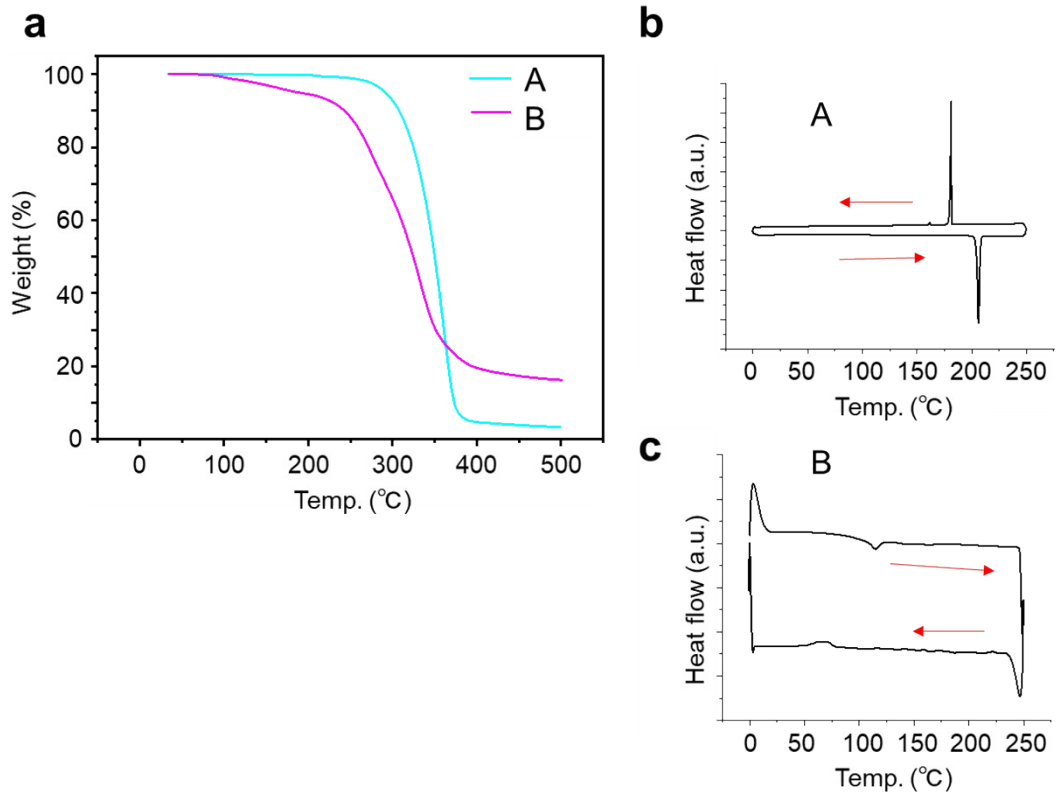

Figure S4. (a) TGA and (b)(c) DSC profiles of crystals **A** and **B**.

Table S3. Thermal properties of the crystal polymorphs

	A	**B**
T_d (°C)[a]	310	265
T_m (°C)[b]	207	110
T_l (°C)[c]	179	68

[a] Thermal degradation temperature was determined with TGA.

[b] Melting temperature was determined with DSC.

[c] Crystallization temperature was determined with DSC.

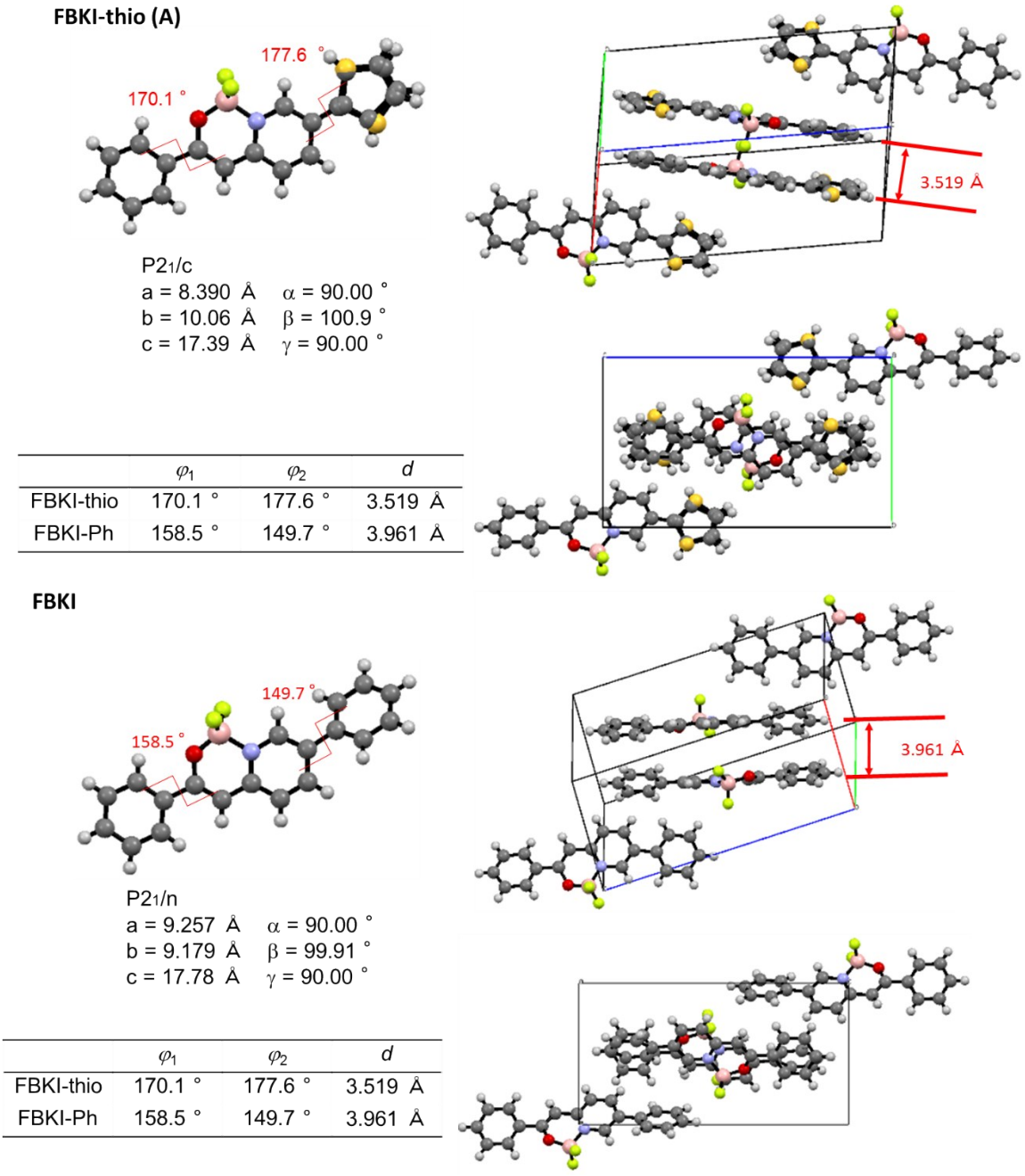

	φ_1	φ_2	d
FBKI-thio	170.1 °	177.6 °	3.519 Å
FBKI-Ph	158.5 °	149.7 °	3.961 Å

	φ_1	φ_2	d
FBKI-thio	170.1 °	177.6 °	3.519 Å
FBKI-Ph	158.5 °	149.7 °	3.961 Å

Figure S5. Comparison of crystal packings between FBKI-thio in crystal **A** and FBKI.

Table S4. Crystallographic data of crystal **A** of FBKI-thio

Empirical formula	C17H12BF2NOS
Formula weight	327.15
Temperature (K)	93
Wavelength (Å)	0.71075
Crystal system, space group	monoclinic, *P21/c*
Unit cell dimension	a = 8.3895(5)
	b = 10.0595(8)
	c = 17.3911(11)
	α = 90.00
	β = 100.872(7)
	γ = 90.00
V (Å)	1441.36(17)
Z, calculated density (g cm^{-3})	4, 1.508
Absorption coefficient	0.249
F(000)	672
Crystal size (mm)	0.250 × 0.200 × 0.160
θ range for date collection	2.025−27.482
Limiting indices	$-10 \le h \le 10$, $-13 \le k \le 13$, $-22 \le l \le 22$
Reflections collected (unique)	13833/11216 [R(int) = 0.0363]
Completeness to theta = 27.485	0.997
Max. and min. transmission	1.0000 and 0.3573
Goodness-of-fit on F^2	1.125
Final R indices [$I > 2\sigma(I)$][a]	R_1 = 0.0679, wR_2 = 0.2019
R indices (all data)	R_1 = 0.0817, wR_2 = 0.2127

[a] $R_1 = \Sigma(|F_0|-|F_c|)/\Sigma|F_0|$. w$R_2 = [\Sigma w(F^2_0-F^2_c)^2/\ \Sigma w(F^2_0)^2]^{1/2}$. $w = 1/[\sigma^2(F^2_0)+[(ap)^2+bp]]$, where $p = [\max(F^2_0,0)+2F^2_c]/3$.

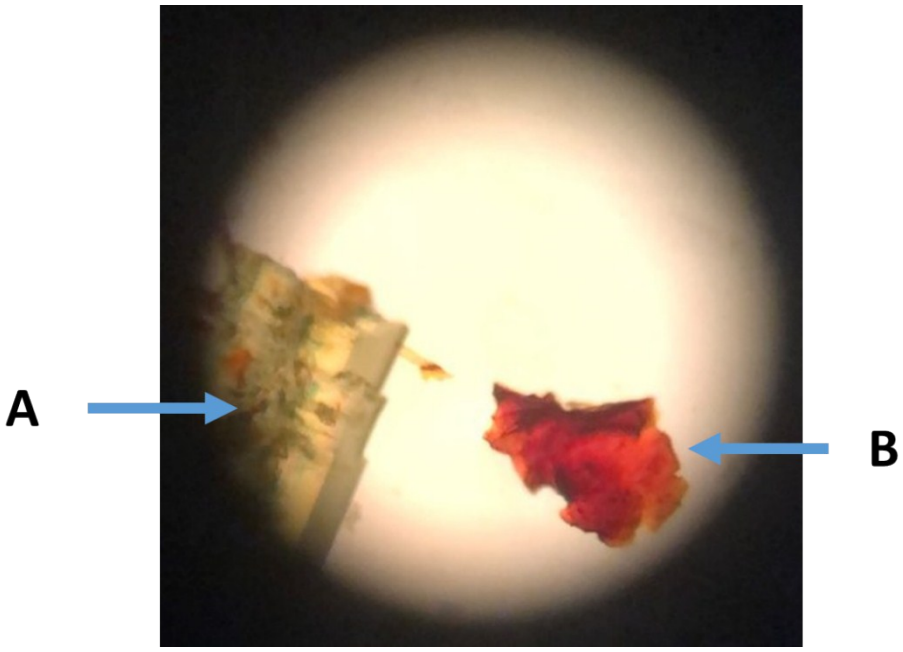

Figure S6. Microscopic observation with both crystals **A** and **B**.

Table S5. Emission on decay times of FBKI-thio before and after the mechanical treatments[a]

sample	Detection (nm)	τ_1 (ns)[b]	τ_2 (ns)[b]	τ_3 (ns)[b]	χ^2
A	500	2.88 (40%)	1.78 (60%)	–	1.07
A-G	500	2.42 (38%)	1.09 (62%)	–	1.04
A-G	487	2.32 (39%)	1.06 (61%)	–	1.12
B	566	1.64 (57%)	0.65 (43%)	–	1.17
B-S	566	4.73 (28%)	1.74 (32%)	0.57 (40%)	1.09
B-S	529	4.34 (40%)	1.84 (28%)	0.54 (32%)	1.04
B-S	490	4.41 (38%)	2.38 (38%)	0.68 (24%)	1.05
B-G	566	5.89 (26%)	1.61 (42%)	0.38 (32%)	1.15
B-G	517	4.72 (30%)	1.43 (38%)	0.44 (32%)	1.10
B-G	491	4.03 (32%)	1.22 (36%)	0.37 (32%)	1.03

[a] Excited at 375 nm.

[b] Proportion of each component is shown in the parentheses.

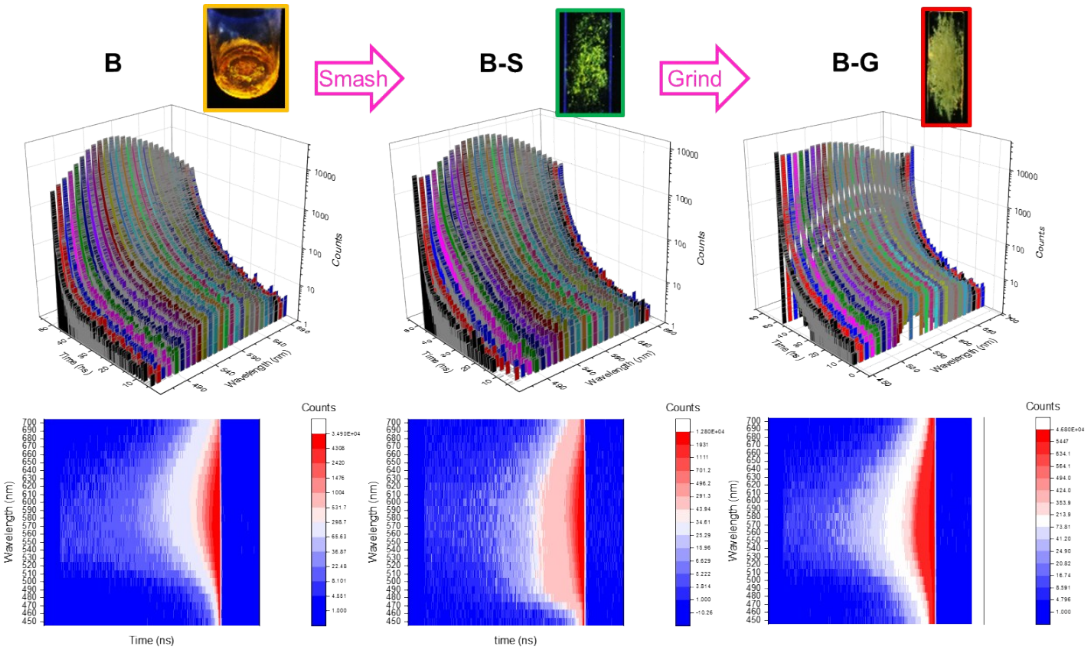

Figure S7. Decay curves by changing detection wavelengths with crystal **B** before and after the mechanical treatments..

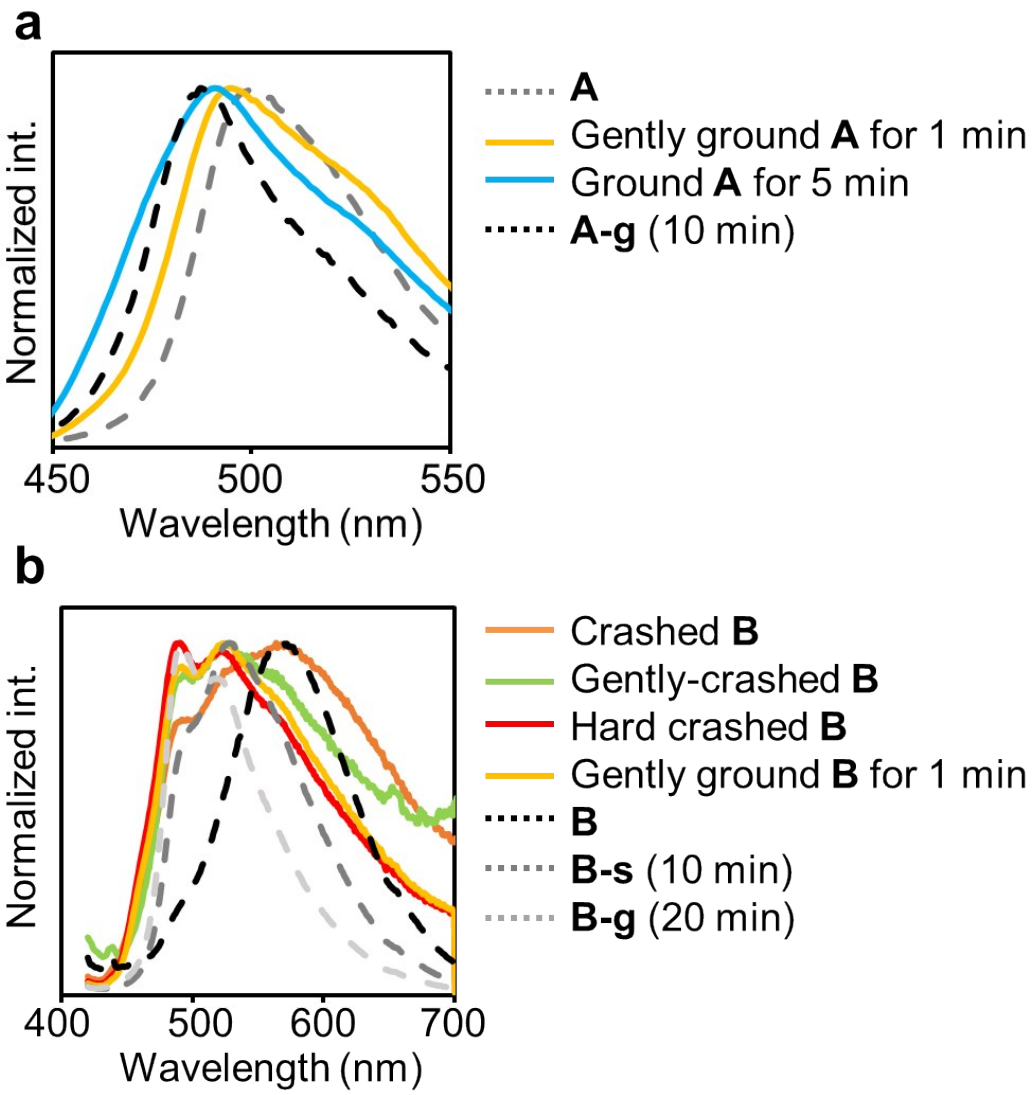

Figure S8. Photoluminescence spectra of (a) **A** and (b) **B** after various mechanical treatments.

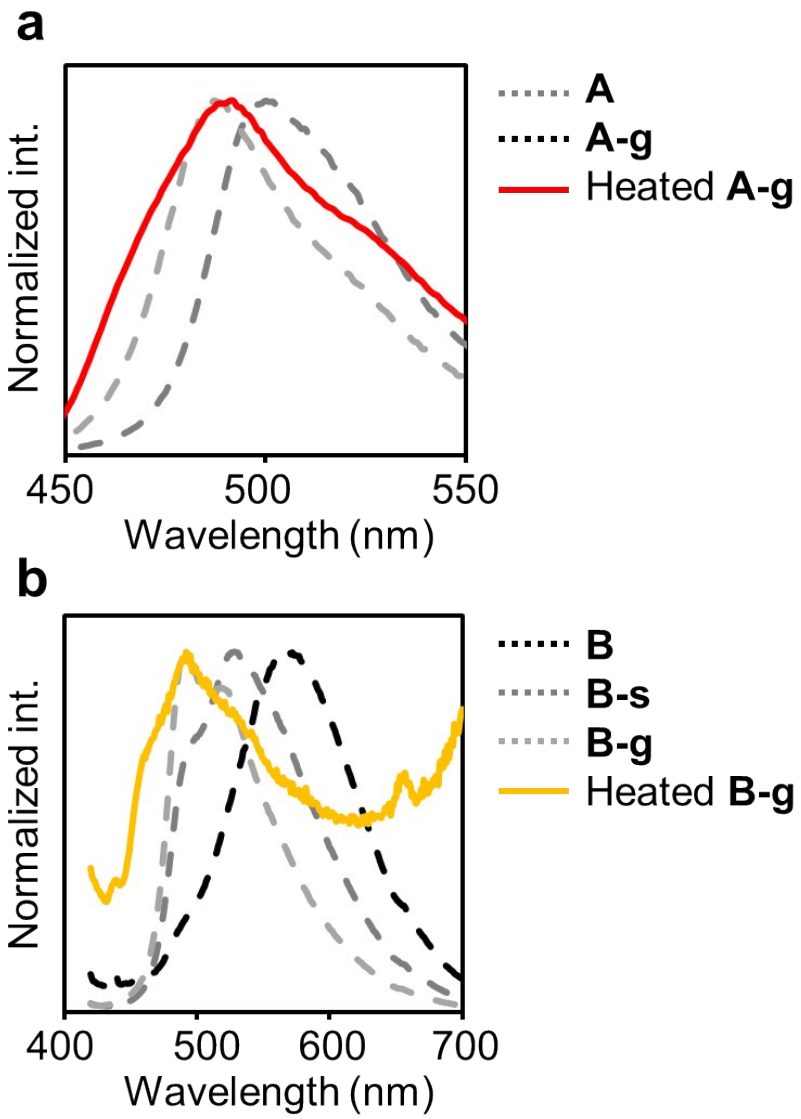

Figure S9. Photoluminescence spectra of (a) **A-g** and (b) **B-g** before and after heating at 80 °C for 1 h.

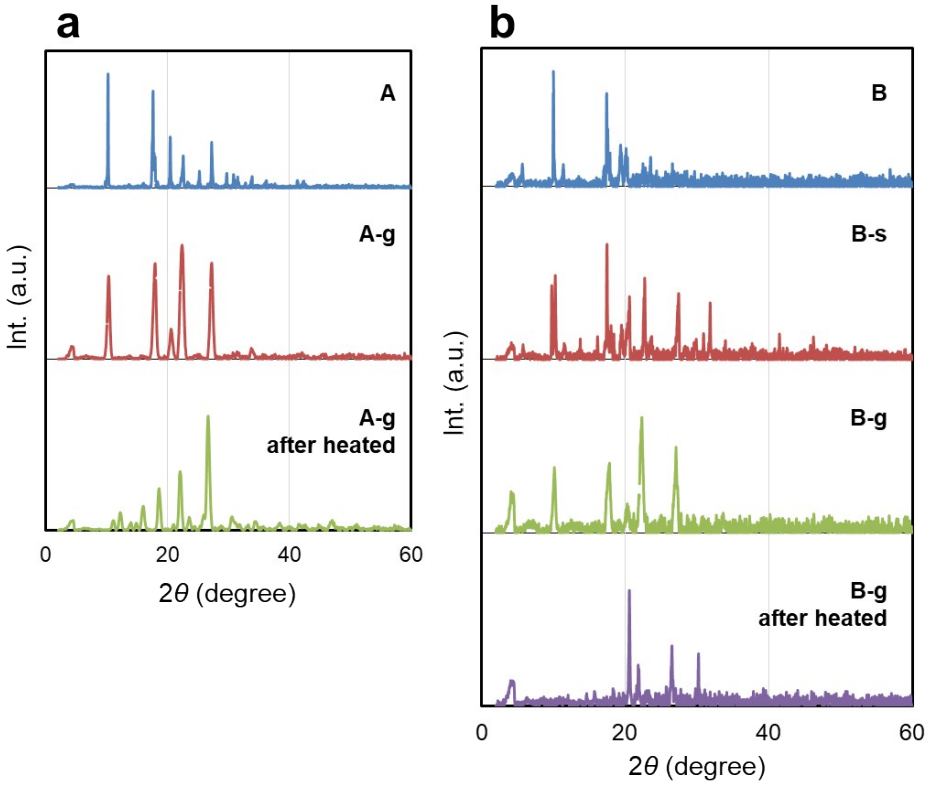

Figure S10. PXRD patterns of (a) **A-g** and (b) **B-g** before and after heating at 80 °C for 1 h.